eNeuro

Research Article: New Research | Sensory and Motor Systems

Neural coding of perceived odor intensity

Coding of odor intensity

Yevgeniy B. Sirotin[1,+], Roman Shusterman[2,3,+] and Dmitry Rinberg[2,4]

[1]*The Rockefeller University, New York, NY, 10065, USA*

[2]*Janelia Farm Research Campus, Howard Hughes Medical Institute, Ashburn, VA, 20147, USA*

[3]*Sagol Department of Neurobiology, University of Haifa, Haifa, 34905 Israel*

[4]*NYU Neuroscience Institute, New York University Langone Medical Center, New York, NY, 10016, USA*

DOI: 10.1523/ENEURO.0083-15.2015

Received: 26 July 2015

Revised: 25 October 2015

Accepted: 28 October 2015

Published: 12 November 2015

Author contributions: Y.B.S., R.S., and D.R. designed research; Y.B.S. and R.S. performed research; Y.B.S., R.S., and D.R. analyzed data; R.S. and D.R. wrote the paper.

Funding: Howard Hughes Medical Institute; Howard Hughes Medical Institute; Leon Levy Foundation; National Institute of Health: 8 UL1 TR000043.

Conflict of Interest: The authors declare no competing financial interests.

[+]Equal Contributions

Corresponding author: Dmitry Rinberg NYU Neuroscience Institute, New York University Langone Medical Center, New York, NY, 10016, USA. rinberg@nyu.edu

Cite as: eNeuro 2015; 10.1523/ENEURO.0083-15.2015

eNeuro

http://eneuro.msubmit.net

eN-NWR-0083-15R1

Neural coding of perceived odor intensity

Title: Neural coding of perceived odor intensity

Abbreviated title: Coding of odor intensity

Author names and affiliations: Yevgeniy B. Sirotin[1+], Roman Shusterman[2,3+], Dmitry Rinberg[2,4*]

[1]The Rockefeller University, New York, NY, 10065, USA

[2]Janelia Farm Research Campus, Howard Hughes Medical Institute, Ashburn, VA, 20147, USA

[3]Sagol Department of Neurobiology, University of Haifa, Haifa, 34905 Israel

[4]NYU Neuroscience Institute, New York University Langone Medical Center, New York, NY, 10016, USA

[+]Equal Contributions

Corresponding author: Dmitry Rinberg NYU Neuroscience Institute, New York University Langone Medical Center, New York, NY, 10016, USA; ***rinberg@nyu.edu***

Number of figures - 9

Number of words

Abstract – **148**
Significance - **120**
Introduction - **704**
Discussion – **1809**

Acknowledgements: We thank Admir Resulaj and Kirin Furst for technical help in performing experiments, Magnus Karlsonn, Tanya Tabachnik, and Pawel Wojcik for design and fabrication of experimental equipment. We thank Cori Bargmann, Thomas Bozza, Leslie Voshall, Alexei Koulakov, Aniruddha Das, Genela Morris, and Matthew Smear for helpful discussions and critical comments.

Conflict of Interest "The authors declare no competing financial interests."

Funding sources: R.S. and D.R. were supported by the Howard Hughes Medical Institute. Y.B.S. was supported by the Leon Levy Foundation and by the Visiting Scientist Program at JFRC. The work is partially supported by grant # 8 UL1 TR000043 from the National Center for Research Resources and the National Center for Advancing Translational Sciences (NCATS), National Institutes of Health to YBS.

Abstract

Stimulus intensity is a fundamental perceptual feature in all sensory systems. In olfaction, perceived odor intensity depends on at least two variables, odor concentration and duration of the odor exposure, or adaptation. To examine how neural activity at early stages of the olfactory system represents features relevant to intensity perception, we studied responses of mitral/tufted cells (MTCs) while manipulating odor concentration and exposure duration. Temporal profiles of MTC responses to odors changed both as a function of concentration and with adaptation. However, despite the complexity of these responses, adaptation and concentration dependencies behaved similarly. These similarities were visualized by principal component analysis of average population responses and quantified by discriminant analysis in a trial-by-trial manner. The qualitative functional dependencies of neuronal responses paralleled psychophysics results in humans. We suggest that temporal patterns of MTC responses in the olfactory bulb contribute to an internal perceptual variable - odor intensity.

Significance Statement

Establishing a link between perception and neural activity is one of the major goals of systems neuroscience. Yet, tracking perceptual variables in animal models where one can perform neural recording remains a challenge. Here we demonstrate a consistency between human perception of odor intensity and activity of mitral/tufted cells (MTCs) recorded in the olfactory bulb of awake mice as a function of two physical variables: odor concentration and the duration of odor exposure. Human perception of odor intensity decreased sharply after just one sniff of odor. Consistently, sniff-locked MTC odor responses changed abruptly after the first sniff so as to mimic responses to lower odor concentrations. We suggest that early processing stages may already contribute to an odor intensity percept.

Introduction

One of the major aims of systems neuroscience is to link neural activity at different stages of information processing with specific aspects of perception. Strong links with perception have been established in the visual and somatosensory systems (Britten et al., 1992; Johnson et al., 2002; Romo et al., 2002), however, such perceptual links are dramatically absent in olfaction (but see (Wilson and Stevenson, 2006)). Despite this, the olfactory system has become an established model for studying neural coding due to its relatively simple, accessible, and evolutionarily conserved organization (Hopfield, 1995; Laurent, 2002; Kepecs et al., 2006; Wilson and Mainen, 2006).

Perhaps the most basic perceptual axis for all senses is stimulus intensity. Intensity is a perceptual variable that facilitates comparisons of different objects within a single modality as well as across modalities (Over and Mackintosh, 1969; Marks, 1978; Wojcik and Sirotin, 2014). In olfaction, intensity is a common feature of all odors (Beck et al., 1954; Engen, 1964) and the perceptual organization of intensity is conserved across the mammalian species (rats and humans). Intensity is related to odor concentration as a power function (Cain, 1969; 1970; Moskowitz et al., 1976; Wojcik and Sirotin, 2014) and intensity discrimination performance is scale invariant (Stone, 1963; Stone and Bosley, 1965; Wojcik and Sirotin, 2014). Even the relationship between intensity and the physicochemical properties of odors appears conserved across species (Edwards and Jurs, 1989; Wojcik and Sirotin, 2014). The conservation of the perceptual properties of intensity in olfaction likely reflects the highly conserved neural processing mechanisms of olfactory systems across species. While it has been shown that neuronal activity in the piriform cortex, entorhinal cortex (Rolls et al., 2003), and amygdala (Anderson et al., 2003) correlate with intensity perception, how neural activity at specific stages in olfactory processing contributes to this perceptual variable is unclear. In rats and humans, odor intensity grows systematically with concentration and rapidly decreases with adaptation (Engen, 1964; Ekman et al., 1967; Cain, 1970; Pryor et al., 1970; Steinmetz et al., 1970; Wojcik and Sirotin, 2014; Cain et al., 1969). Thus, perceived intensity for a given odor is a function of at least two variables: the physical odor concentration and the sampling duration. Therefore, in order for a neuronal response to underlie odor intensity coding, it should change consistently

with concentration and sampling duration. In the current work we will exploit this consistency in order to reveal the relationship between neuronal responses and a perceptual variable.

Mitral/tufted cells (MTCs), in the olfactory bulb have been a subject of multiple studies due to their central role in the processing of olfactory information. MTCs are the only cells that transmit information from the bulb to higher brain areas. They receive primary input from individual glomeruli, and their processing is affected by other glomeruli via lateral interactions. In awake animals, where the dynamics of these cell is very different from that in anesthetized state (Rinberg, 2006; Kato et al., 2012), olfactory information is encoded by MTCs activity at sub-sniff times scale (Cury and Uchida, 2010; Shusterman et al., 2011). Moreover, recent work demonstrated that these fine temporal patterns can be read by higher brain areas (Smear et al., 2011; 2013), thus establishing connection between coding properties of MTC and their role in behavior. Our knowledge about concentration and adaption dependencies of these cells is mostly based on recordings from anesthetized animals (Chalansonnet and Chaput, 1998; Wilson, 1998) but see (Patterson et al., 2013). Here we explore both concentration and adaptation dependencies of MTCs in awake mice and their potential role in forming the intensity percept.

In mammals, the flow of odor to the olfactory epithelium is controlled by the breathing/sniffing rhythm (Kepecs et al., 2006). This rhythm sets the natural time scale of odor processing to the duration of a single inhalation/exhalation ('sniff') cycle. Based on experiments in rodents, the structure and the temporal scale of information encoding in the olfactory system (Cury and Uchida, 2010; Shusterman et al., 2011) is consistent with behavioral results that 1-2 sniffs are sufficient for olfactory decision making (Uchida and Mainen, 2003; Abraham et al., 2004; Rinberg et al., 2006). Here we compare concentration and adaptation dependencies of MTCs with human odor intensity perception, both measured on sniff based time scales.

Methods

Neural recording

Animals. Data were collected in four C57BL/6J mice. Mice were 6–8 weeks old at the beginning of behavioral training and were maintained on a 12-h light/dark cycle (lights on at 8:00 p.m.) in isolated cages in a temperature- and humidity-controlled animal facility. All animal care and

experimental procedures were in strict accordance with a protocol approved by the Authors Institutional Animal Care and Use Committee.

Electrophysiology. MTC spiking activity was recorded using 32-channel Si-probes (NeuroNexus, model: a4x8-5mm-150-200-312 (H32)). Cells were recorded in both ventral and dorsal mitral cell layers. The identity of MTCs was established on the basis of criteria formulated in previous work (Rinberg, 2006). The data were acquired using a 32-channel data acquisition system (Digital Lynx, NeuraLynx) with widely open broadband filters (0.1–9,000 Hz) and sampling frequency of 32.556 kHz.

Sniff recording. To monitor the sniff signal, we implanted a thin 7-mm-long stainless cannula (gauge 23, Small Parts capillary tubing) in the nasal cavity. The cannula was capped between experimental recordings. During experiments, the cannula was connected to a pressure sensor with polyethylene tubing (801000, A-M Systems). The pressure was measured with a pressure sensor (MPX5050, Freescale Semiconductor) and homemade preamplifier circuit. The signal from the preamplifier was recorded together with electrophysiological data on one of the data acquisition channels. The sniff monitor was calibrated against a known flow as described in (Shusterman et al., 2011). The lag between the pressure zero crossing and airflow velocity zero crossing was below 1 ms.

Surgery. Mice were anesthetized using isoflurane gas anesthesia. The horizontal bar for head fixation, pressure cannula and electrode chamber were implanted during a single surgery. To implant the sniffing cannula, a small hole was drilled in the nasal bone, into which the cannula was inserted and affixed with glue and stabilized with dental cement. To implant the electrode chamber, a small craniotomy (~1 mm^2) was done above the left or right olfactory bulb. After the insertion of the Si-probe, the electrode chamber was fixed by dental cement to the skull, posterior to the olfactory bulb. The reference electrode was implanted in the cerebellum. The mice were given at least 5 days after a surgery for recovery.

Behavioral procedure and training. After recovery, the mice were placed in the head-fixation setup. The first few sessions were brief (10–20 min) and served to acclimate the animals to head fixation in the setup. Mice typically remained mostly quiescent after 1–2 sessions of head fixation, after which odor sessions started. We delivered 1 of 4 odors at three concentrations in pseudo-random sequence with an average inter-stimulus interval of 7 s and stimulus duration of

144 at least 2sec. One session usually lasted for ~1.5 to 3 hours and contained 600-1200 trials (50 to
145 100 trials per stimulus).

146 *Odor delivery.* For stimulus delivery we used a nine-odor air dilution olfactometer. The airflow
147 through the selected odorant vial was diluted ten times by the main airflow stream and
148 homogenized in a long thin capillary before reaching the final valve. It took approximately 500–
149 1,000 ms to prepare the homogenized mixture and equilibrate the concentration. A steady stream
150 of 1,000 ml min^{-1} of clean air was flowing to the odor port at all times except during stimulus
151 delivery, when the flow from the olfactometer was directed to the odor port. After sufficient
152 mixing and equilibration time, the final valve (four-way Teflon valve, NResearch) switched the
153 odor flow to the odor port, and diverted the clean airflow to the exhaust. All flows and line
154 impedances were tuned to minimize the pressure shock resulting from line switching and
155 minimize the time of odor concentration stabilization after opening the final valve. Temporal
156 odor concentration profile was checked by mini-PID (Aurora Scientific). The concentration
157 reached a steady state ~40 ms after final valve opening.

158 Odor delivery was triggered on the end of the inhalation phase of the sniff cycle, which was
159 detected by positive-going zero crossings of the pressure signal. This prevents odor from being
160 delivered at random times during inhalation, which would confound our analysis. Furthermore,
161 as no odor enters the nose during exhalation phase, this allows enough time for the odor stimulus
162 to reach a steady state of concentration by the time the animal begins inhaling.

163 We used multiple odorants obtained from Sigma-Aldrich. The odorants were stored in liquid
164 phase (diluted 1:5 in mineral oil) in dark vials. The odorant concentration delivered to the animal
165 was reduced an additional tenfold by air dilution. The following odorants were used:
166 acetophenone, amyl acetate, behzaldehyde, butyric acid, decanol, ethyl acetate, ethyl tiglate, 1-
167 hexanol, hexanoic acid, hexanal, 2-hexanone, hexyl acetate, R-limonene, isopropyl tiglate,
168 methyl benzoate, methyl salicylate, 1-octanol and 2-undecanone.

169 All of the analysis discussed below was performed in Matlab (MathWorks).

170 *Spike extraction.* Acquired electrophysiological data were filtered and spike sorted using a
171 WaterShed software package written by Alexei Koulakov.

Temporal warping. Sniffing recordings were down-sampled to 1 kHz, and filtered in the range of 0.5–20 Hz. Initially, the times of inhalation onset and offset were detected by negative and positive zero-crossings, respectively. Often the positive zero-crossing at the end of inhalation phase was not well defined, owing to the very shallow slope of the signal. To more reliably estimate the offset of the inhalation phase, we fit a parabola to the minima of the pressure signal following the onset of the inhalation (Shusterman et al., 2011). Inhalation offset was defined as the second zero crossing of the parabola. We defined two intervals: the first is from inhalation onset to inhalation offset and the second is the rest of the sniffing cycle, from the inhalation offset to the next inhalation onset. For the whole session, we estimated an average duration for both intervals. Each interval of the sniffing data, together with correspondent spiking data, was stretched or compressed to make its duration equal to the duration of the average interval. For analysis, we used only sniffs of typical duration (between 200 and 500 ms), which constitute ~80% of all sniffs. Analysis of odor responses was restricted to the first 200 ms of response following sniff onset in warped time coordinates.

Odor responses. We compared the distributions of the neuronal activity with and without odors. Neuronal activity without odor was sampled from sniffs preceding odor delivery across all trials. Neuronal activity for a given odor was sampled from the first sniff after stimulus onset for the trials containing a correspondent odor delivery. Units were considered responsive if their spike probability statistically differed from the distribution of baseline responses (randomly subsampled) in at least one 10 ms bin relative to inhalation onset ($p<0.005$) or if their average spike rate over the sniff cycle differed significantly from baseline ($p<0.05$). Responses were considered initially excitatory (inhibitory) if the earliest statistically significant deviation of the response after sniff onset for the highest odor concentration was an increase (decrease) in spike rate or, if no single bin was statistically significant, and a mean firing rate increased (decreased) following odor onset (Fig. 1A). Sharp responses were defined using previously established criteria (Shusterman et al., 2011).

Quantifying response parameters for individual unit-odor pairs. To examine how responses of individual unit-odor pairs changed with odor concentration and adaptation, we constructed PSTH traces for different odor concentrations and for different sniffs following odor onset. We filtered the response using a 10 ms sliding boxcar window with a 1 ms step. For a given sniff, we defined the following parameters: average firing rate (FR) – the mean firing rate during the sniff;

peak amplitude (A) – the peak of the PSTH for the sniff; peak latency (L) – the time, relative to sniff onset, of the PSTH peak. Figure 1C plots the distribution of latency and amplitude on the first sniff for all significant responses.

To examine how response timing changed with concentration, we measured the relative latency from the lag in cross-correlation functions between PSTHs for first sniff responses to the high concentration and for the lower concentration, $\Delta L^1_{0.3-1.0}$. This enabled us to use a common measure for both positive and negative responses as well as for responses without a well-defined peak. For sharp responses, the relative latency was strongly correlated with the difference in peak latency for the two concentrations (Fig. 2). Positive values of $\Delta L^1_{0.3-1.0}$ correspond to delayed responses at lower concentrations. To examine changes in amplitude, ΔA and firing rates, ΔFR, we subtracted values for the high concentration from values for the lower concentration to obtain $\Delta A^1_{0.3-1.0} = A^1_{0.3} - A^1_{1.0}$ and $\Delta FR^1_{0.3-1.0} = FR^1_{0.3} - FR^1_{1.0}$.

For adaptation, we performed similar analyses, but with responses to the high concentration on the seventh sniff replacing responses for the lower concentration on the first sniff. Thus, positive values of $\Delta L^{7-1}_{1.0}$ correspond to delayed responses following adaptation. We also computed changes in amplitude and firing rate as: $\Delta A^{7-1}_{1.0} = A^7_{1.0} - A^1_{1.0}$ and $\Delta FR^{7-1}_{1.0} = FR^7_{1.0} - FR^1_{1.0}$.

To determine if response changes following odor dilution were correlated with response changes following adaptation over the population of recorded unit-odor pairs, we computed Spearman cross correlations between ΔL, ΔA, and ΔFR values obtained for changes in concentration and with adaptation. Calculations were made separately for excitatory, inhibitory, and sharp responses.

Population response vectors. To examine patterns of neuronal activity, for every cell k ($k = 1,..M_{unit}$), at trial i ($i = 1,...N$, where N=50-100), sniff s ($s = -1,1,..7$), and time bin t ($t = 1,..T$), we defined the response as a number of spikes in a given bin: $S^k_{s,i}(t)$. We constructed the following vectors:

average firing rate of cell k at sniff s trial i:

$$\bar{r}^k_{s,i} = \frac{1}{T}\sum_{t=1}^{T} S^k_{s,i}(t),$$

229 average firing rate across trials:

$$\bar{R}_s^k = \frac{1}{N}\sum_{i=1}^{N} \bar{r}_{s,i}^k,$$

230 temporal pattern of cell k at sniff s at trial i (spike count at a given bin minus average firing
231 rate):

$$r_{s,i}^k(t) = S_{s,i}^k(t) - \bar{r}_{s,i}^k,$$

232 and trial averaged temporal pattern:

$$R_s^k(t) = \frac{1}{N}\sum_{i=1}^{N} r_{s,i}^k(t).$$

233 *Principal component analysis.* To examine the principal sources of variability in our data set, we
234 performed principal components analysis (PCA) on population response vectors (PRVs) for cell-
235 odor pairs recorded across 3 odor concentrations of odor (M=49 cell-odor pairs). The firing rate
236 PRV for each concentration and each sniff (total 21 vectors) consists of firing rates of individual
237 cell-odor pairs: $\mathbf{R}_s = [\bar{R}_s^1, \bar{R}_s^2, \ldots \bar{R}_s^M]$, while temporal PRV is composed of concatenated of trial
238 averaged PSTHs (200 ms per sniff, binned at 10 ms: T=20 time-points per cell) for each sniff and
239 each concentration for all cell odor pairs: $\mathbf{T}_s = [R_s^1(1), R_s^1(2), \ldots R_s^1(T), R_s^2(1) \ldots R_s^M(T)]$. PCA
240 was performed using the *svd.m* function in MATLAB. The first three principal components
241 accounted for the bulk of the variance in the responses. Reduced population vectors were
242 created by reconstructing the population vector using only the first three PCs. To visualize
243 changes across vectors, we projected each response onto the first three principal components
244 from the analysis (Fig. 5).

245 To examine the robustness of PCA solution, we split single trial responses for each unit-odor-
246 concentration combination into 10 non-overlapping sets and created 10 sets of PRVs from the
247 resulting PSTHs. We then projected these PRVs into the space of the 3 PCs generated from
248 average PRVs and computed standard deviation ovals within the space of the first and second
249 and second and third PC (Fig 4, small markers, shaded ovals).

250 *Classifier analysis.* To classify single trial population vectors for each sniff s, and each
251 concentration, $c \in \{0, 0.1, 0.3, 1.0\}$, we constructed a Euclidean distance classifier that classified

each vector $\mathbf{r}_{s,c,i} = \left[r_{s,i}^{1}(1), r_{s,i}^{1}(2), \ldots r_{s,i}^{M}(T)\right]_c$ as belonging to the group with an average population vector $\mathbf{R}_{s,c} = [R_s^1(1), R_s^1(2), \ldots R_s^M(T)]_c$ for a given sniff and concentration: that was closest to it in the full neural response space according to:

$$D\left(\mathbf{r}_{s,c,i}, \mathbf{R}_{s,c}\right) = \left[\sum_{k=1}^{M}\sum_{t=1}^{T}\left(r_{s,c,i}^{k}(t) - R_{s,c}^{k}(t)\right)^2\right]^{\frac{1}{2}}$$

Single trial population vectors were created by randomly selecting a single trial response pattern for each unit out of a pool of recorded single trial responses. This procedure was repeated 250 times for different single trial population vectors. The selected single trial responses were excluded from trial averaged vectors. Figure 5 shows classification between trial averaged and single trial vectors on the same sniff: $\mathbf{r}_{s,c,i} \rightarrow \left\{\mathbf{R}_{s,0}, \mathbf{R}_{s,0.1}, \mathbf{R}_{s,0.3}, \mathbf{R}_{s,1.0}\right\}$. Figure 6 shows classification between single trial vectors on different sniffs and trial averaged vectors on the first sniff: $\mathbf{r}_{\mathbf{s,c,i}} \rightarrow \left\{\mathbf{R}_{1,0}, \mathbf{R}_{1,0.1}, \mathbf{R}_{1,0.3}, \mathbf{R}_{1,1.0}\right\}$. The trial averaged vector for the blank response $\mathbf{R}_{\mathbf{s,0}} = \langle \mathbf{R}_{-1,c} \rangle$ was included all classifications.

Human psychophysics

Subjects. Subjects were screened using a comprehensive questionnaire to establish that they had normal olfactory function. Volunteers completed three visits to become acquainted with performing computer-controlled olfactory tasks and then 4-8 visits on which perceptual data was collected. Three volunteers (2 males, 1 female; ages 24-31) participated in the study. All experiments were approved by the Institutional Review Board.

Odor delivery. Experiments were conducted using a custom-built air dilution olfactometer modeled after (Bodyak and Slotnick, 1999). Briefly output of an air compressor (Easy Air, Precision Medical) was charcoal filtered (Vacu-Guard 150/Activ. Carbon, Whatman) and split into three pressure regulated lines. One of the lines labeled 'clean' carried 20 L/min of filtered air directly to the subject. Flow in the other two lines was digitally controlled by two mass flow controllers (Alicat Scientific) that regulated their combined flow to 2 L/min. These connected into upstream and downstream teflon manifolds of the olfactometer. Air flowing into the upstream manifold could be directed to one of eight vials containing pure odorant by solenoid pinch valves (BioChem Valve; Neptune Research). Odorized air was then combined with clean

air in the upstream manifold. Odor concentration could be controlled by changing the ratio of odorized to clean air (odorized air flow 0-0.3 L/min, clean air flow 2-1.7 L/min). To minimize effects of odor absorption, all tubing (1-2 mm ID) after the odor vial was made of Teflon. Air from the olfactometer was combined with the 20 L/min clean air stream using an additional custom Teflon manifold that terminated in a Teflon coated mask shaped to fit the human nose (Nasal Ranger). The exhaust port of the mask was routed to a pair of mass flow sensors (AWM720P1, Honeywell) that measured inhalations and exhalations (typical peak flow rates of 50 L/min). Stable odor output and fast kinetics of the olfactometer were confirmed frequently using a photoionization detector (mini-PID, Aurora Scientific). The olfactometer (solenoid opening; changes in odor flow rate) was controlled by a custom-made circuitry and software powered by a PC running MATLAB (MathWorks) interfacing with an Arduino Mega 1280 microcontroller.

Task. Volunteers sat facing a gray computer screen with their nose inside the odor port and hands placed on the number pad of a keyboard. Initiation of a trial was queued by two brief beeps and a message on the computer screen instructing them to prepare for sniffing. Volunteers were then instructed to make a series of inhalations and exhalations queued by tones (2 sec duration). The first inhalation in the series had no odor and served to entrain the subjects' breathing. Subjects then inhaled an adapting odor concentration (60 ml/min saturated vapor delivered in 22 L/min air) for 0-3 inhalations. After the adaptation period, flow rate of the odor was changed to one of six test values (0, 15, 30, 60, 120, and 300 ml/min). After making one inhalation of the test concentration, subjects were instructed to rate its perceived intensity on a scale of 0-9. Each trial was separated by a 30 second inter-trial-interval to reduce the effect of trial-to-trial adaptation.

To calibrate volunteers' perceptual scale, they performed several test runs where they were presented with the full range of odor concentrations used in the study without adaptation. They were asked to assign 9 for the highest concentration and 0 for no odor. The relative ratings of the intermediate concentrations were at the discretion of the volunteers.

All manipulations were repeated for two odors: isoamyl acetate and α-pinene. One volunteer did not adapt to α-pinene, possibly due to lower overall perceived intensity of this odor and was excluded from analysis of that odor. In each session volunteers performed 5 repetitions for each stimulus condition used (4 adaptation durations x 6 concentrations = 24 conditions) resulting in

120 trials per session (total duration = 1.5 hours). To obtain stable estimates of perceived intensity, subjects repeated the experiment 2-5 times, resulting in N = 10-50 intensity ratings for each stimulus condition.

Data Analysis. Data for each trial consisted of sniffing traces and numerical perceived intensity ratings. For each subject, we pooled perceived intensity estimates across all sessions and took the mean of perceived intensity for each condition. Average perceived intensity across volunteers was then computed as the mean of average perceived intensity estimates for each volunteer.

We estimated the relationship between perceived intensity and concentration without adaptation by fitting Hill equations of the form (Chastrette et al., 1998):

$$I = \frac{I_m C^n}{C_{\text{ip}}^n + C^n}$$

where I is the perceived intensity, C is the concentration, n is the hill coefficient, I_m is the maximum intensity rating, C_{50} is the concentration at the inflection point. The fits were performed independently for each subject.

Effective concentration was calculated independently for each subject by finding the concentration that best matches the perceived intensity of the stimulus after adaptation from the fitted Hill equation.

Results

Our data set comprises recordings from putative MTCs (total 134 units, 47 single units, 87 multi-units) and breathing/sniffing signals from four awake head-fixed mice, passively sampling one of a few presented odors at 2 or 3 different concentrations (total 209 unit-odor pairs, and 548 unit-odor-concentration combinations). Based on our previous work, in order to analyze the odor responses at sniffs of different durations, we applied the sniff-warping technique, by stretching or compressing the temporal intervals corresponding to inhalation and the rest of the sniff cycle to their mean values (Shusterman et al., 2011). We generated sniff-warped traces of activity (see methods) for each unit, each odor, and each concentration, of the odor stimuli (peri-sniff-time-histograms; PSTH; Fig. 1A).

MTC responses change with concentration

To quantify response changes as function of odor concentration we first grouped responses into 339 unit-odor-concentration sets (concentration-response sets, CRSs). Each CRS consists of responses to two presented concentrations with a 3x fold concentration difference (two CRSs for each unit-odor pair if 3 concentrations were presented, and one CRS if 2 concentrations were presented). The CRSs were divided into initially excitatory (86, 25%), initially inhibitory (89, 26%) responses (henceforth excitatory and inhibitory) and sharp responses (29, 9%), a subset of responses, which exhibit large rapid changes in firing rate (Shusterman et al., 2011) (Fig. 1 A, B; see Methods). Each CRS was assigned one of the three response types (excitatory, inhibitory, and sharp) based on the response at the highest concentration measured on the first sniff. For each type we characterized the responses and response changes with concentration by estimating their latencies, amplitudes and average firing rates (see methods).

In contrast to recordings in the anesthetized state, in awake mice the spontaneous MTC firing rate is relatively high (19-[12,24] Hz, here and further: median-[25-75% inter quartile range(IQR)]), which precludes estimation of latency by the timing of the first spike in response to a stimulus (Cang and Isaacson, 2003; Margrie and Schaefer, 2003). Thus we estimated absolute response latency as the timing of the maximum/minimum of PSTH for the excitatory/inhibitory responses.

Excitatory responses: Over the population of all presented concentrations of all odors, excitatory responses tiled the sniff cycle: their peak latencies on the first sniff varied from 52 ms to 270 ms after inhalation onset (Fig.1C). The peak amplitudes of the responses (48-[33,67] Hz) were not distributed uniformly across the sniff cycle, with responses in the highest quartile ($\geq$ 67 Hz, n = 38 responses) coming earlier (median latency, 90 ms) relative to responses falling into lowest quartile ($\leq$ 33 Hz, n = 33) - 137 ms ($p < 0.001$, Wilcoxon rank sum test for equal medians). Responses in the highest quartile were predominantly sharp (25 of 38), but none of the lowest quartile responses were sharp.

We next examined how the latency, amplitude, and firing rates of responses changed with odor concentration (Fig.1C and Methods). For the population of 86 excitatory CRSs, reducing odor concentration decreased peak amplitudes by 7.8 Hz (median, $p < 0.001$), and decreased net firing rates by 1.2 Hz (median, $p < 0.001$). Responses to lower concentrations were delayed by a

relative latency of 2.9 ms (median, $p<0.001$ Wilcoxon signed rank test for zero median) compared to high concentration responses. This relative latency shift was estimated from the time shift of the peak of the cross correlation function between the responses at the two concentrations. This method was used to avoid errors in estimation of differences in PSTH latency and to create a measure that can be used for both excitatory and inhibitory (see below) responses. Latency changes were particularly apparent for sharp responses, which had median delays of 7.5 ms. For sharp responses, direct estimation of the latency change yielded 9.4-[0.4, 19.4] ms. (Fig. 2). These latency changes are smaller than previously reported for first spike latency in anesthetized animals (50 msec shift for a 10-fold dilution (Cang and Isaacson, 2003)), but this could be due to different measures of response latency change (relative or absolute latency vs. time of first spike) and different sniffing patterns in awake and anesthetized states.

Inhibitory responses: For inhibitory responses, decreasing odor concentration increased the firing rates at the peak of the inhibitory response ($p<0.001$, median increase = 0.2 Hz) and increased the overall firing rate ($p<0.001$, median increase = 2.4 Hz). However, for inhibitory responses, decreasing concentration did not significantly alter relative response latency. These results are consistent with previous data showing enhanced responses of inhibitory cells in the olfactory bulb with increased odor concentration, which may account for the greater inhibition at higher concentrations observed here (Cang and Isaacson, 2003).

Early and late responses: Early and late odor responses may play different role in concentration coding because they may be generated by different cell classes (Fukunaga et al., 2012). To test this hypothesis, we divided response distributions into early (<100 ms after inhalation onset) and late (>100 ms after inhalation onset; Fig. 1D). Only excitatory responses (but not sharp excitatory) had statistically significant differences between early and late response distributions. For early excitatory responses, the mean latency change was larger than for late: 7.3 ms vs 1.5 ms ($p=0.01$) and the mean firing rate change was smaller: 0.51 Hz vs 1.38 Hz.

Adaptation mimics the effect of decreased concentration on fine temporal responses of MTCs

We next compared changes of MTC responses resulting from adaptation following repeated odor sampling. For this analysis, we created adaptation response sets (ARSs), in which we paired the higher concentration response from each CRS on the first sniff to responses of the same MTC on

the seventh sniff of the same concentration. We then analyzed these ARSs in the same manner as the above CRS analysis.

Excitatory responses: Adaptation significantly reduced the amplitude of excitatory responses and increased the relative response latency in a manner similar to a decrease in concentration (Fig. 3). For sharp responses, adaptation decreased the amplitude of peak responses by 12.6 Hz (median, $p<0.001$), which was associated with a significant reduction in overall firing rates by 4.2 Hz (median, $p<0.001$). Adaptation also delayed excitatory responses by 4.1 ms (median, $p<0.001$). Again, latency changes were most pronounced for sharp responses with median delays of 15.3 ms estimated using cross correlation and 23.9 ms by direct comparison of latencies.

Importantly, excitatory response changes induced by adaptation were correlated to changes observed with odor dilution (Fig. 4). We found a significant correlation between the relative latency ($\rho= 0.45$, $p<0.001$) and changes in the amplitude ($\rho = 0.31$, $p = 0.004$) of odor responses, as well as the average firing rate ($\rho = 0.25$, $p = 0.022$).

Inhibitory responses: For inhibitory responses, adaptation increased the peak firing rate by 0.25 Hz (median, $p < 0.001$) and the overall firing rate by 1.3 Hz (median, $p = 0.002$). Adaptation also tended to delay inhibitory responses by 0.8 ms (median, $p = 0.018$). For inhibitory responses, changes in response timing and amplitude, but not spike rate were significantly correlated between adaptation and concentration (Fig. 4).

Early and late responses: As for concentration dependencies, we compared changes in response adaptation for early and late responses (defined above; Fig.3C). For excitatory responses (but not sharp excitatory) there were significant differences in the adaptation induced mean response latency change (11.5 ms vs 2.6 ms, early vs late, $p = 0.04$) and in the mean amplitude change (25.6 Hz vs 11.4 Hz, $p <0.001$). For inhibitory responses early and late responses differed by the change in amplitude (0.0Hz vs 2.2 Hz, $p<0.001$), and firing rate (-0.7 Hz vs -4.7 Hz, $p< 0.001$). No significant differences were observed between early and late sharp responses.

Total spike count unlikely to explain intensity coding

Whereas the temporal activity patterns changed in suggestively similar ways with odor dilution and adaptation, similarity in total spike count (a gross measure of neural activity) was much less

compelling. We first counted the total number of spikes in the first sniff observed for different concentrations across all units on a single trial. While some units either increased or decreased their spike counts with concentration, there was little change in total spike count over the full population. Increasing odor concentration tended to decrease the average net spike count: 4.4±0.3 spikes per sniff cycle pre odor to 3.9±0.3 spikes for the highest concentration but this change was not statistically reliable ($p=0.09$; Fig. 5A). Adaptation increased spike count, but again not reliably (Fig. 5B). Thus, it is doubtful that the total level of activity is a reliable code for odor intensity (Chalansonnet and Chaput, 1998; Stopfer et al., 2003).

Adaptation and concentration move population response vectors along a common trajectory in PC space

Odor intensity is likely encoded by the spatiotemporal pattern of activity across many cells in the olfactory bulb (Stopfer et al., 2003; Bathellier et al., 2008). Prior studies have suggested that the temporal pattern of MTC activity is consistent with odor based perceptual decisions (Cury and Uchida, 2010). We reasoned that, to be consistent with perception, changes in response patterns from the first sniff to subsequent sniffs should resemble changes observed with odor dilution. To examine how intensity is represented by the temporal activity profile our population of MTCs, we combined our population of unit-odor pairs into population response vectors (PRVs) by concatenating the recorded unit responses. We made separate PRVs for different concentrations and different sniff numbers. To track population response trajectories along a larger concentration range, we used only sessions where odors were presented at 3 different concentrations: 0.1, 0.3, and 1.0 relative to maximal concentration (67 concentration response sets, one set for each unit-odor pair; see methods). Thus we have 22 different PRVs: 21 vectors for 3 concentrations and 7 consecutive sniffs, and 1 vector for non-odorized sniff. Each coordinate of these vectors is a deviation of the single trial spike rate from the average spike rate across sniff for one out of 67 unit-odor pairs and one out of 20 time bins during a sniff cycle (total 67x20=1340 coordinates). We then examined how PRVs changes with concentration and with adaptation.

To identify the most meaningful dimensions of the response patterns across concentration and sniff number, we reduced the dimensionality of these 22 1340-dimensonal vectors using principal components analysis (PCA). We visualized responses on each sniff and concentration

by plotting the responses in the space of the first three principal components (PCs), which accounted for 70% of the total variance (Fig. 6A-B).

Changes in PRVs with concentration and adaptation were consistent with a representation of odor intensity. PRVs moved smoothly with concentration, creating a curved trajectory away from baseline pre odor responses in PC space. Both concentration and adaptation moved PRVs along roughly the same trajectory in the space of the first two PCs (Fig. 6A). In this way, responses after adaptation aligned with responses for lower concentrations on the first sniff.

Interestingly, after adaptation the distance between PRVs for different concentration became smaller while response variability remained similar (Fig. 6A). This suggests that individual concentrations should be more difficult to identify following adaptation.

The consistency with intensity was not observed for population responses composed only of the average firing rates. (Fig. 6C-D). We performed PCA for response vectors where each coordinate was the average firing rate over a sniff cycle for one out of 67 unit-odor pairs. Increasing concentration moved these vectors away from baseline in PC space. Adaptation moved firing rate PRVs in a direction different from concentration decrease. Thus, though both concentration and adaptation changed the pattern of firing rates, their effects on the response were not consistent and therefore not obviously related to intensity coding.

Visual inspection of PCA results provides qualitative intuition for two hypotheses: it predicts that 1) adaptation increases errors in concentration discrimination, and 2) adaptation decreases encoded odor concentration. To test these hypotheses quantitatively, we performed single trial discriminant analysis of MTC population responses. In addition we examine the perceptual implications of the above hypotheses by measuring the effect adaptation and concentration change on human intensity perception.

Single trial discriminant analysis

Animals make decisions based on odor information available in a single trial. We estimated how much information is carried by spatiotemporal pattern of MTC activity in single trial in the first and subsequent sniffs using discriminant analysis (see Methods). As for PCA, we used sessions in which three different concentrations were presented (67 unit-odor pairs). We considered all unit-odor pairs independent and equivalent to different cell responses to one odor.

Adaptation increases errors in identifying odor concentrations.

On the first sniff a single responsive MTC can, on average, identify the presented concentration level (0.0, 0.1, 0.3, or 1.0) at 31% accuracy, which is slightly higher than chance (25%). However, identification accuracy quickly increased as more units were included in the analysis, reaching 92% for the maximal number of recorded unit-odor pairs (n=67) (Fig.7A). With a single unit, the average probabilities of misidentifying a given concentration as 3x or even 10x different were nearly equal. Increasing the number of units in the analysis abolished errors to 10x and, the analysis using maximal number of units nearly abolished errors to 3x concentration differences. This means that most classification errors are made to adjacent concentrations in a manner consistent with a graded code for concentration. To capture this effect, we estimated the concentration identification noise, σ, as the width of a Gaussian fit to our classification results as a function of concentration difference (in log units), $\Delta log(C)$: $p = p_1 exp\left(-\left(\Delta log_{10}(C)\right)^2/\sigma^2\right)$ (Fig.7A). For a single MTC, the average concentration identification noise was equal to 1.63 (corresponding to a 43-fold concentration difference), decreasing to just 0.3 log units (2-fold) for our full population of responses (Fig. 7A inset).

We next examined classifier performance after adaptation using our full population of responses. Correct identification performance decreased from 92% on the first sniff to 68-78% on subsequent sniffs (Fig. 7B), while identification noise increased from 0.3 to 0.4 log units (2.6-fold concentration difference; t-test, p = 0.048; Fig. 7B, inset). As for the first sniff, misidentification errors on later sniffs occurred between similar concentrations.

Thus, although concentration information was still largely intact after adaptation, odor concentrations were harder to distinguish as suggested earlier by PCA.

Adaptation reduces coded odor concentration.

Our PCA analysis suggested that responses to odors following adaptation should become more similar to lower odor concentrations. Using discriminant analysis we classified responses on consecutive sniffs for a given concentration based on their similarity to the average responses on the first sniff at different concentrations (Fig. 8) As predicted, responses on later sniffs were preferentially matched to lower, but rarely to higher concentrations. For each presented concentration on each sniff we estimated the 'effective' concentration, as the best matching

concentration on the first sniff. To do this we computed the sum of the presented concentrations weighted by the match probability between a given sniff-concentration response and concentration responses on the first sniff (0.1, 0.3, 1.0) and also baseline (conc. = 0). This measure of effective concentration decreased abruptly after the first sniff and quickly reached a steady state corresponding to a 3 to 10-fold lower concentration (Fig. 8).

Adaptation reduces perceived intensity ratings, increasing rating noise

To further develop our understanding of the relationship between adaptation and concentration changes we performed psychophysical experiments with human subjects. We asked human volunteers to rate the perceived intensity of odors across sniffs. We measured perceived intensity of odors across several consecutive inhalations in three subjects (Fig. 9). Volunteers were asked to rate a panel of odor concentrations presented either on the first sniff or after several sniffs of an adapting concentration. In general agreement with prior work (Moncrieff, 1957; Engen, 1964; Cain, 1970; Stone et al., 1972), average intensity ratings followed a non-linear relationship with odor concentration well described by the Hill equation (Chastrette et al., 1998) (odor isoamyl acetate; Fig. 9A). We quantified trial-to-trial variability of perceived intensity ratings as a function of the presented concentration. To do this, we computed rating noise as the ratio of the standard deviation of intensity ratings relative to their mean (Fig 9D). Rating noise decreased significantly with odor concentration. For isoamyl acetate, rating noise decreased on average across subjects from 0.59 ± 0.16 (mean ± standard deviation) at the lowest concentration to 0.07 ± 0.02 at the highest.

Prolonged exposure to a constant odor source decreased mean intensity ratings (33 ± 0.02% decrease for isoamyl acetate). Converting from intensity to concentration units using the fitted Hill equation showed that these lower ratings corresponded to a roughly 2-fold dilution of the odor (methods, Fig. 9C). Whereas the mean of the perceived intensity ratings decreased with adaptation, the rating noise increased from 0.34±0.02 to 0.52±0.10. We observed similar effects across different odors (see Methods). These results of human psychophysics experiments are consistent with observations made from MTC responses: namely that the effective concentration of odors quickly decreases after the first sniff with an associated increase in identification noise.

Discussion

Here we investigated the neural representation of odor intensity in the olfactory bulb of awake mice. We find that MTC odor responses change similarly with decreasing concentration as with repeated sampling of a constant odor source. We used our recorded population of MTCs to decode odor concentration using classifier analysis. On the first sniff, MTCs reliably identified the presented odor concentration to within a factor of 2, but identification noise increased on later sniffs. Using first sniff responses to classify concentrations on later sniffs resulted in poor performance because responses on later sniffs were systematically misclassified as lower concentrations. These neural results are consistent with changes in perceived odor intensity across sniffs reported by human volunteers. Repeated sampling of a constant odor source caused a decline of perceived intensity ratings and an associated increase in rating noise. Our data suggest that responses of neurons in the olfactory bulb are consistent with the perceptual feature of odor intensity.

A representation of odor intensity on each sniff

Rodents and humans can make decisions based on a single sniff of odor(Laing, 1986; Uchida and Mainen, 2003; Kepecs et al., 2006). This implies that animals' olfactory percept is regenerated, or at least refreshed, on each sniff by the incoming pattern of MTC activity. Thus, a constant odor source does not present a static input into the olfactory system but is converted, by sniffing, into discrete samples. Consistent with prior studies, we find that the pattern of MTC activity on each individual sniff carries a robust code for odor concentration (Gross-Isseroff and Lancet, 1988; Chalansonnet and Chaput, 1998; Bathellier et al., 2008; Zhou and Belluscio, 2012; Patterson et al., 2013). This code has been shown to change significantly with repeated sampling, reducing the ability of classifiers to correctly identify the presented concentration when using the first sniff as a response template (Bathellier et al., 2008; Patterson et al., 2013).

We find that reduced classification accuracy observed across sniffs is not due to random drifts in the neural response over time, but rather systematic decreases in the coded odor concentration. Over the population of recorded MTCs, the peak response amplitude, response latency, and firing rate changed from the first to subsequent sniffs. Further, these response changes were significantly correlated with how responses change with odor dilution. Principal component analysis of MTC population responses illustrated that concentration and adaptation have similar

trajectories in PC space, with responses after adaptation becoming systematically more similar to responses to lower concentrations. Finally whereas our classifier analysis quantitatively confirmed prior findings of reduced classification accuracy between sniffs, this effect was dominated by classification errors to 3x to 10x lower odor concentrations. These data suggest that each sniff of a constant odor source generates a new odor percept with perceived intensity falling immediately after the first sniff.

Though most of the variability in MTC responses could be attributed to changes in odor intensity, responses after adaptation were also significantly different from any of the responses on the first sniff. These differences were clearly captured by the third principal component in our PC analysis (Fig. 4B), suggesting that perceptual properties other than intensity (e.g. odor quality) change in different ways with adaptation as compared to concentration.

Early and late responses do not show difference in intencity coding.

Prior work proposed that responses of Tufted and Mitral cells have different concentration dependence (Fukunaga et al., 2012). In the anesthetized state, odor responses of Tufted cells peaked early after inhalation onset and had very small latency shifts with concentration, whereas the Mitral cells responded late and had a much greater shifts in latency with concentration. Our recordings in the awake state did not show a similar relationship between early and late responses and their latency shifts with concentration, and do not allow us to differentiate cell types. Therefore, our data cannot determine whether Mitral and Tufted cells participate differently in intensity coding.

Possible mechanisms for similar MTC responses changes for adaptation and concentration decrease.

At the receptor level, adaptation and concentration have different effects. Increasing odor concentration usually leads to recruitment of a larger number of olfactory receptor neurons (ORNs) (Bozza et al., 2004; Grosmaitre, 2006). Prior work shows that increasing odor concentration can increase ORN spike counts and reduce response latency (Duchamp-Viret et al., 2000). Strong peripheral adaptation at the level of OSNs was reported for high concentrations of odor, while responses to lower odor concentration where mainly unaltered (Lecoq et al., 2009). This effect may explain change in perception of odor identity for high concentrations and may be unrelated to perception of odor intensity. Investigations in humans attempted to relate receptor

activity to perception of intensity using electro-olfactograms (EOGs), a measurement reflecting mass action of olfactory receptors. Despite good correlation between changes of EOG amplitudes with concentration and changes in perceived intensity with concentration (Lapid et al., 2009), the two measures were dissociated by adaptation. While perceived intensity was greatly reduced by repeated odor sampling, EOG amplitudes remained virtually unchanged (Hummel et al., 1996). This casts doubt on receptor based explanations of perceived intensity based on pooled receptor response magnitudes. Alternatively, feedback within OB or from higher olfactory areas may alter odor representation after the first sniff of odor (Patterson et al., 2013), which could mimic the concentration decrease. In addition, granule cells, which show little response modulation by respiration in awake state (Cazakoff, 2014), may be a good candidate for suppressing and delaying responses across sniffs.

Responses following adaptation are compressed along the intensity axis

Our finding of a 3x to 10x drop in the odor concentration coded by populations of MTCs in mice is strikingly similar to the decrease in perceived odor intensity measured in rats (Wojcik and Sirotin, 2014) and humans ((Engen, 1964; Ekman et al., 1967; Cain, 1970; Pryor et al., 1970; Steinmetz et al., 1970; Wojcik and Sirotin, 2014; Cain et al., n.d.); and data herein). Wojcik and Sirotin found that the relative perceived intensity of an odor following adaptation falls by a factor 3x to 10x following a brief 300 ms exposure depending on odor type. This adaptation period corresponds to roughly two sniffs. Even a single sniff of odor in human volunteers was sufficient to decrease the perceived odor intensity by a factor of 2x. Thus, decreases in perceived intensity are generally consistent with changes in concentration coding at the level of MTCs.

In addition to a decrease in the coded odor concentration, classifier analysis of MTC responses showed that later sniffs were associated with a greater number of errors (identification noise) compared to the first sniff. There are two possible explanations of this result: an increase in the variability of intensity responses on later sniffs or constant variability but with adapted responses closer together along the intensity axis. Our PCA showed that responses after adaptation moved closer to lower concentration responses, but were not significantly more variable. Perceptual data from human volunteers showed that the across-trial variability in intensity ratings was constant across the full range of mean rated intensity. This caused intensity rating noise to increase with decreasing stimulus intensity. Decreases in intensity with adaptation were also

accompanied by increased rating noise. This finding is consistent with responses following adaptation being compressed along the intensity axis while the noise in the represented concentration remains fixed.

Which features of the neural response carry intensity information?

Although our results demonstrate that neural responses of MTCs are broadly consistent with a representation of odor intensity, all examined features of MTC activity changed in similar ways with concentration and adaptation. Of the examined features, the relationship was weakest for changes in mean firing rate across the sniff cycle and PCA of the firing rate pattern across MTCs did not show any systematic links between response changes with concentration and adaptation. However, because any of the examined neural features can likely be read out behaviorally and may influence perception (Smear et al., 2013), it is difficult to assign any one a causal role. Prior works have suggested a number of ways in which odor intensity may be represented in the olfactory bulb (Koulakov et al., 2007; Schaefer and Margrie, 2007; Zhou and Belluscio, 2012). In the future, these plausible theories can be tested using targeted trial-by-trial perturbations of neural activity combined with perception in the same animals.

Comparing olfactory perception across species

Despite dramatic phylogenetic differences, general principles of olfactory structure and coding appear conserved among mammals, fish, and insects. In all species, axons from olfactory sensory neurons are pooled into glomeruli where they synapse onto principal neurons (MTCs in mammals and fish, PN in insects) embedded in an inhibitory network. In all systems examined, these principal neurons respond to odors with spatiotemporal activity patterns (Laurent, 2002) that refine the odor representation before sending it to higher brain areas (Mori, 1999; Friedrich and Laurent, 2001). Because of such structural and functional homology across phyla, it is likely that neural mechanisms of odor coding are also conserved.

In this study we compared perceptual adaptation in humans with MTC odor responses in awake mice. Despite significant differences in sampling behavior (0.25 Hz sniffing in humans; 3 Hz sniffing in mice), the magnitude and even the fast kinetics of adaptation appear comparable across species (Smith et al., 2010; Wojcik and Sirotin, 2014). We monitored neural data across seven sniffs of odor by mice, which correspond to over two seconds of odor exposure, similar to one human inhalation. Odor adaptation in olfactory sensory neurons can be long-lasting(Zufall

659 and Leinders-Zufall, 2000; Patterson et al., 2013). Thus the drop in perceived intensity of on the
660 second inhalation of odor in our volunteers may indeed be mediated by neural mechanisms
661 similar in quality to the observed changes in mouse MTC responses. We suggest that the insight
662 gained from measuring human perception can serve as a synergistic tool for understanding neural
663 representations and coding in olfaction (Zelano and Sobel, 2005) just as these comparisons have
664 been useful in understanding other sensory modalities (Mountcastle et al., 1963; Johnson et al.,
665 2002).

666 Relating olfactory perception to neural responses can help elucidate how and where odor
667 percepts are represented in the olfactory system. In other systems, this approach led to
668 significant insight into the representation of perceptual features (Mountcastle et al., 1963; Britten
669 et al., 1996; Hernández et al., 2000; Yoshioka et al., 2001; Liu et al., 2012). One idea that has
670 been put forth is that any candidate neural code for a specific perceptual feature must show
671 consistency with perception (Johnson et al., 2002). Here we demonstrate that the sniff triggered
672 temporal pattern of neural responses in the olfactory bulb changes in a similar manner with odor
673 dilution and adaptation, showing qualitative consistency with the perceptual phenomenon of
674 adaptation. It may be useful to apply this approach to investigating links between other
675 perceptual and neurophysiological phenomena, such as olfactory afterimages (Patterson et al.,
676 2013) or masking (Cain, 1975).

References

Abraham NM, Spors H, Carleton A, Margrie TW, Kuner T, Schaefer AT (2004) Maintaining accuracy at the expense of speed: stimulus similarity defines odor discrimination time in mice. Neuron 44:865–876.

Anderson AK, Christoff K, Stappen I, Panitz D, Ghahremani DG, Glover G, Gabrieli JDE, Sobel N (2003) Dissociated neural representations of intensity and valence in human olfaction. Nat Neurosci 6:196–202.

Bathellier B, Buhl DL, Accolla R, Carleton A (2008) Dynamic Ensemble Odor Coding in the Mammalian Olfactory Bulb: Sensory Information at Different Timescales. Neuron 57:586–598.

Beck A, Kruger L, Calabresi P (1954) Observations on olfactory intensity. I. Training procedure, methods, and data for two aliphatic homologous series. Annals of the New York Academy of Sciences 58:225–238.

Bodyak N, Slotnick B (1999) Performance of mice in an automated olfactometer: odor detection, discrimination and odor memory. Chemical Senses 24:637–645.

Bozza T, McGann JP, Mombaerts P, Wachowiak M (2004) In vivo imaging of neuronal activity by targeted expression of a genetically encoded probe in the mouse. Neuron 42:9–21.

Britten KH, Newsome WT, Shadlen MN, Celebrini S, Movshon JA (1996) A relationship between behavioral choice and the visual responses of neurons in macaque MT. Vis Neurosci 13:87–100.

Britten KH, Shadlen MN, Newsome WT, Movshon JA (1992) The analysis of visual motion: a comparison of neuronal and psychophysical performance. J Neurosci 12:4745–4765.

Cain WS (1969) Odor intensity: Differences in the exponent of the psychophysical function. Percept Psychophys 6:349–354.

Cain WS (1970) Odor intensity after self-adaptation and cross-adaptation. Attention, Perception, & Psychophysics 7:271–275.

Cain WS (1975) Odor intensity: mixtures and masking. Chemical Senses 1:339–352.

Cain WS, Engen T, (1969) Olfactory adaptation and the scaling of odor intensity. In: Olfaction and Taste III (Pfaffmann C, ed), pp 127–141. Rockefeller University Press, New York.

Cang J, Isaacson JS (2003) In vivo whole-cell recording of odor-evoked synaptic transmission in the rat olfactory bulb. Journal of Neuroscience 23:4108–4116.

Cazakoff BN, Lau BYB, Crump KL, Demmer HS, Shea SD (2014) Broadly tuned and respiration-independent inhibition in the olfactory bulb of awake mice. Nat Neurosci 17:569–576.

711 Chalansonnet M, Chaput MA (1998) Olfactory bulb output cell temporal response patterns to
712 increasing odor concentrations in freely breathing rats. Chemical Senses 23:1–9.

713 Chastrette M, Thomas-Danguin T, Rallet E (1998) Modelling the human olfactory stimulus-
714 response function. Chemical Senses 23:181–196.

715 Cury KM, Uchida N (2010) Robust Odor Coding via Inhalation-Coupled Transient Activity in
716 the Mammalian Olfactory Bulb. Neuron 68:570–585.

717 Duchamp-Viret P, Duchamp A, Chaput MA (2000) Peripheral odor coding in the rat and frog:
718 quality and intensity specification. J Neurosci 20:2383–2390.

719 Edwards PA, Jurs PC (1989) Correlation of odor intensities with structural properties of
720 odorants. Chemical Senses 14:281–291.

721 Ekman G, Berglund B, Berglund U, Lindvall T (1967) Perceived intensity of odor as a function
722 of time of adaptation. Scandinavian journal of psychology 8:177–186.

723 Engen T (1964) PSYCHOPHYSICAL SCALING OF ODOR INTENSITY AND QUALITY.
724 Annals of the New York Academy of Sciences 116:504–516.

725 Friedrich RW, Laurent G (2001) Dynamic optimization of odor representations by slow temporal
726 patterning of mitral cell activity. Science 291:889–894.

727 Fukunaga I, Berning M, Kollo M, Schmaltz A, Schaefer AT (2012) Two distinct channels of
728 olfactory bulb output. Neuron 75:320–329.

729 Grosmaitre X, Vassalli A, Mombaerts P, Shepherd GM, Ma M (2006) Odorant responses of
730 olfactory sensory neurons expressing the odorant receptor MOR23: a patch clamp analysis in
731 gene-targeted mice. Proc Natl Acad Sci USA 103:1970–1975.

732 Gross-Isseroff R, Lancet D (1988) Concentration-dependent changes of perceived odor quality.
733 Chemical Senses 13:191–204.

734 Hernández A, Zainos A, Romo R (2000) Neuronal correlates of sensory discrimination in the
735 somatosensory cortex. Proc Natl Acad Sci USA 97:6191–6196.

736 Hopfield JJ (1995) Pattern recognition computation using action potential timing for stimulus
737 representation. Nature 376:33–36.

738 Hummel T, Knecht M, Kobal G (1996) Peripherally obtained electrophysiological responses to
739 olfactory stimulation in man: electro-olfactograms exhibit a smaller degree of desensitization
740 compared with subjective intensity estimates. Brain Res 717:160–164.

741 Johnson KO, Hsiao SS, Yoshioka T (2002) Neural coding and the basic law of psychophysics.
742 The Neuroscientist : a review journal bringing neurobiology, neurology and psychiatry
743 8:111–121.

744 Kato HK, Chu MW, Isaacson JS, Komiyama T (2012) Dynamic sensory representations in the
745 olfactory bulb: modulation by wakefulness and experience. Neuron 76:962–975.

746 Kepecs A, Uchida N, Mainen ZF (2006) The sniff as a unit of olfactory processing. Chemical
747 Senses 31:167–179.

748 Koulakov A, Gelperin A, Rinberg D (2007) Olfactory coding with all-or-nothing glomeruli.
749 Journal of Neurophysiology 98:3134–3142.

750 Laing DG (1986) Identification of single dissimilar odors is achieved by humans with a single
751 sniff. Physiology & Behavior 37:163–170

752 Lapid H, Shushan S, Plotkin A, Voet H, Roth Y, Hummel T, Schneidman E, Sobel N (2011)
753 Neural activity at the human olfactory epithelium reflects olfactory perception. Nat Neurosci
754 14:1455–1461.

755 Laurent G (2002) Olfactory network dynamics and the coding of multidimensional signals. Nat
756 Rev Neurosci 3:884–895.

757 Lecoq J, Tiret P, Charpak S (2009) Peripheral adaptation codes for high odor concentration in
758 glomeruli. J Neurosci 29:3067–3072.

759 Liu S, Gu Y, Deangelis GC, Angelaki DE (2013) Choice-related activity and correlated noise in
760 subcortical vestibular neurons. Nat Neurosci.16:89-97

761 Margrie TW, Schaefer AT (2003) Theta oscillation coupled spike latencies yield computational
762 vigour in a mammalian sensory system. The Journal of Physiology 546:363–374.

763 Marks L (1978) The unity of the senses. Academic.1978

764 Moncrieff RW (1957) Olfactory adaptation and odor-intensity. The American Journal of
765 Psychology 70:1–20.

766 Mori K (1999) The Olfactory Bulb: Coding and Processing of Odor Molecule Information.
767 Science 286:711–715.

768 Moskowitz HR, Dravnieks A, Klarman LA (1976) Odor intensity and pleasantness for a diverse
769 set of odorants. Attention, Perception, & Psychophysics 19:122–128.

770 Mountcastle VB, Poggio GF, Werner G (1963) The Relation of Thalamic Cell Response to
771 Perepherial Stimuli Varied over an Intensive Continuum. Journal of Neurophysiology
772 26:807–834.

773 Over R, Mackintosh NJ (1969) Cross-modal transfer of intensity discrimination by rats. Nature
774 224:918–919.

775 Patterson MA, Lagier S, Carleton A (2013) Odor representations in the olfactory bulb evolve
776 after the first breath and persist as an odor afterimage. Proceedings of the National Academy
777 of Sciences.110: E3340-9

778 Pryor GT, Steinmetz G, Stone H (1970) Changes in absolute detection threshold and in
779 subjective intensity of suprathreshold stimuli during olfactory adaptation and recovery.
780 Attention, Perception, & Psychophysics 8:331–335.

781 Rinberg D (2006) Sparse Odor Coding in Awake Behaving Mice. Journal of Neuroscience
782 26:8857–8865.

783 Rinberg D, Koulakov A, Gelperin A (2006) Speed-Accuracy Tradeoff in Olfaction. Neuron
784 51:351–358.

785 Rolls ET, Kringelbach ML, de Araujo IET (2003) Different representations of pleasant and
786 unpleasant odours in the human brain. Eur J Neurosci 18:695–703.

787 Romo R, Hernández A, Zainos A, Lemus L, Brody CD (2002) Neuronal correlates of decision-
788 making in secondary somatosensory cortex. Nature Publishing Group 5:1217–1225.

789 Schaefer AT, Margrie TW (2007) Spatiotemporal representations in the olfactory system. Trends
790 in Neurosciences 30:92–100.

791 Shusterman R, Smear MC, Koulakov AA, Rinberg D (2011) Precise olfactory responses tile the
792 sniff cycle. Nat Neurosci 14:1039–1044.

793 Smear M, Resulaj A, Zhang J, Bozza T, Rinberg D (2013) Multiple perceptible signals from a
794 single olfactory glomerulus. Nat Neurosci.

795 Smear M, Shusterman R, O'Connor R, Bozza T, Rinberg D (2011) Perception of sniff phase in
796 mouse olfaction. Nature 479:397–400.

797 Smith DW, Gamble KR, Heil TA (2010) A Novel Psychophysical Method for Estimating the
798 Time Course of Olfactory Rapid Adaptation in Humans. Chemical Senses 35:717–725.

799 Steinmetz G, Pryor GT, Stone H (1970) Olfactory adaptation and recovery in man as measured
800 by two psychophysical techniques. Percept Psychophys.

801 Stone H (1963) Determination of odor Deifference Limens for Three Compounds. J Exp Psychol
802 66:466–473.

803 Stone H, Bosley JJ (1965) Olfactory Discrimination and Weber's Law. Perceptual and motor
804 skills 20:657–665.

805 Stone H, Pryor GT, Steinmetz G (1972) A comparison of olfactory adaptation among seven
806 odorants and their relationship with several physicochemical properties. Attention,
807 Perception, & Psychophysics 12:501–504.

808 Stopfer M, Jayaraman V, Laurent G (2003) Intensity versus identity coding in an olfactory
809 system. Neuron 39:991–1004.

810 Uchida N, Mainen ZF (2003) Speed and accuracy of olfactory discrimination in the rat. Nat
811 Neurosci 6:1224–1229.

812 Wilson DA (1998) Habituation of odor responses in the rat anterior piriform cortex. Journal of
813 Neurophysiology 79:1425–1440.

814 Wilson DA, Stevenson RJ (2006) Learning to Smell: Olfactory Perception from Neurobiology to

815 Behavior. Baltimore: The John Hopkins University Press.

816 Wilson RI, Mainen ZF (2006) Early events in olfactory processing. Annu Rev Neurosci 29:163–
817 201.

818 Wojcik PT, Sirotin YB (2014) Single Scale for Odor Intensity in Rat Olfaction. Curr Biol.

819 Yoshioka T, Gibb B, Dorsch AK, Hsiao SS, Johnson KO (2001) Neural coding mechanisms
820 underlying perceived roughness of finely textured surfaces. J Neurosci 21:6905–6916.

821 Zelano C, Sobel N (2005) Humans as an Animal Model for Systems-Level Organization of
822 Olfaction. Neuron 48:431–454.

823 Zhou Z, Belluscio L (2012) Coding Odorant Concentration through Activation Timing between
824 the Medial and Lateral Olfactory Bulb. Cell Rep.

825 Zufall F, Leinders-Zufall T (2000) The cellular and molecular basis of odor adaptation. Chemical
826 Senses 25:473–481.

827

828

Figure Legends

Figure 1. MTC responses change with odor concentration. A. Sniff warped raster and PSTH plots of sharp excitatory (I-cyan), excitatory (II-brown), and inhibitory (III-green) responses of individual MTCs for 3-fold and 10-fold changes in odor concentration (shown as color shades). Top: Schematic sniff waveform. Gray shading: inhalation. Gray trace: activity of the MTC during blank sniffs. Vertical dashed lines indicate the beginning and end of inhalation interval. **B**. Distribution of different response types observed in the data. **C**. Scatter plot comparing amplitude and latency of sharp, excitatory and inhibitory responses (color notations as in B). Boxplots show marginal response distributions: circle is median, thick line is inter-quartile range (IQR: 25-75% interval), thin lines on either side extend to 1.5*IQR beyond the 25% and 75% quartiles or the farthest data point, whichever is smaller. **D**. Normalized distributions of changes of latencies (left column), amplitude (central column) and firing rate (right column) with 3-fold concentration change across cells for different response types (color notations as in B). Colored asterisks denote significance of test for zero median (* = $p < 0.05$, ** = $p < 0.01$, *** = $p < 0.001$; Wilcoxon rank sum test). In black solid and dashed lines shown distributions for the response latencies for early (<100 ms) and late (>100 ms) responses correspondingly. Black asterisks denote significance of test between two distributions. Arrow marks position of the median.

Figure 2. A. Latency of the first spike estimated using distributions of inter-spike intervals (Shusterman et al., 2011) for responses identified as sharp pooled across all odors and concentrations versus the latency of the peak PSTH for the same response. **B.** Difference in absolute PSTH latency between sharp responses to high and 3x lower concentrations versus the relative latency estimated using cross correlation (see methods).

Figure 3. MTC responses change with repeated sampling. A. Sniff warped raster and PSTH plots of sharp excitatory (I), excitatory (II), and inhibitory (III) responses of single MTCs during 1st, 4th and 7th sniff cycle (shown as color shades). Schematic of sniff waveform is shown above

858 the plots. Gray shading and vertical dashed lines delineate inhalation period. Gray trace: activity
859 of the M/T cell during unodorized sniffs. **B.** Scatter plot comparing amplitude and latency of
860 excitatory, sharp, and inhibitory responses on the seventh sniff following odor onset. Boxplots
861 show marginal response distributions as in Fig. 1C. Color conventions as in Fig 1. **C.** Colored
862 lines are normalized distributions of changes in latency, amplitude and firing rate of sharp,
863 excitatory and inhibitory responses with adaptation (difference between 1st and 7th sniff). Black
864 solid and dashed lines are the same distributions for early and late responses. Notations are same
865 as in Fig. 1D.

866

867 **Figure 4. Correlated changes in response features for concentration and adaptation.** From
868 left to right, plots show changes in the latency, amplitude, and mean firing rate. Points are
869 individual response sets. Response types indicated by color as in Fig. 1. Box plots show
870 distributions of response changes across cells for concentration and adaptation. Conventions as
871 in Fig. 1. Reported r-values are Spearman correlation coefficients computed independently for
872 the three response types. Black arrows mark positions of the three example cells in Fig. 1 and
873 Fig. 2.

874

875 **Figure 5. Spike count unlikely to code odor intensity. A.** Average number of spikes observed
876 on a single sniff for each unit as a function of odor concentration. **B.** Average number of spikes
877 per sniff per cell observed on each sniff for the three tested concentrations and baseline (black =
878 baseline, green = 0.1, red = 0.3; blue = 1.0). Error bars are standard deviation across trials.

879

880 **Figure 6. Principal component analysis of the population vector changes with concentration**
881 **and adaptation. A-B.** The full temporal population vectors plotted in the space of the first and
882 second (**A**) and second and third (**B**) principal components. Large symbols: average PC
883 projection of all first (black) and seventh (gray) sniffs. Small symbols: projection of 10
884 independent subsets of the full data set (shaded ovals: standard deviation). Blank is cross
885 symbol, concentration 0.1, 0.3, and 1.0 are circles, squares, and triangles. Black lines connect
886 first sniffs of different concentrations. Gray lines connect 1st and 7th sniff of the same

887 concentration. Numbers denote presented concentrations. **C-D.** Same as **A-B**, but for average
888 firing rate population vector.

889

890 **Figure 7. Adaptation increases concentration identification error. A**. Results of classification
891 analysis for concentration discrimination between 4 levels (0.0, 0.1, 0.3, 1.0): average probability
892 of classification (empty circles) of temporal patterns of MTCs at the first sniff as a function of
893 concentration mismatch between actual concentration and classified concentration (1
894 corresponds to correct classification, 3(10) is classification mismatch for 1(2) steps concentration
895 differences of 3 fold) for different number of cells (shading from lightest to darkest corresponds
896 to: 1, 2, 4, 8, 16, 32, and 67 cells). Solid lines are Gaussian fits of classification probability:
897 $p=p1\exp(-(\Delta\log10(C))2 \ / \ \sigma2)$, where p1 is a probability of correct classification, σ is
898 concentration classification error in log10 units. Insert: Concentration classification error as a
899 function of number of cells included in classification. Vertical dashed line: 3-fold concentration
900 difference. **B**. Classification performance for all 67 cells for different sniffs following odor onset
901 (black: sniff 1, gray: sniffs 2-7). Inset: Concentration classification error for sniff 1 (black) vs.
902 later sniffs (gray). Dashed line: median for sniffs 2+.

903

904 **Figure 8. Adaptation decreases the encoded odor concentration.** Single trial responses were
905 classified based on their Euclidean distance to the average responses to the three concentrations
906 presented on the first sniff and the average blank response. **A.** Schematics of the classification
907 process for three concentrations (left – 0.1, middle – 0.3, right – 1.0). Responses on a given sniff
908 and concentration (examples are shown in boxes) are classified against responses on the first
909 sniff. The arrows from sniff #5 (shaded box) illustrate match probabilities between this sniff and
910 responses on the first sniff. **B.** For each concentration (left to right), gray scale plots show
911 classifier match probability (see bar on right) for responses on a given sniff (x-axis) with the
912 average concentration responses on the first sniff (y-axis). **C.** Equivalent concentration for each
913 sniff calculated as the average match probability weighted by concentration (circles), and
914 distributions of classification results: thin line is 10-90% interval and thick lines 25-75% interval.

915

Figure 9. Effect of adaptation on perceived odor intensity. A. Average intensity ratings for different concentrations of the odor pinene obtained on the first sniff (black) and after adaptation (gray). Curve denotes average Hill equation fit between concentration and perceived intensity. Concentration has been normalized such that concentration = 1 corresponds to 60 ml/min saturated vapor diluted in a typical 2 second inhalation, peak flow rate 50 L/min (minimum 0.12% saturated vapor). Inset shows rating noise (rating standard deviation / mean). **B.** Perceived intensity of the odor stimulus with concentration = 1 across sniffs from a constant odor source. **C.** Equivalent concentration computed as the concentration with the same intensity rating on the first sniff extrapolated from the Hill equation fit for individual subjects (schematized by dashed gray lines). Error bars are standard deviation across subjects included in the analysis. **D.** Rating noise as a function of presented odor concentration for pinene (dashed) and isoamyl acetate (solid).

Figure 1.

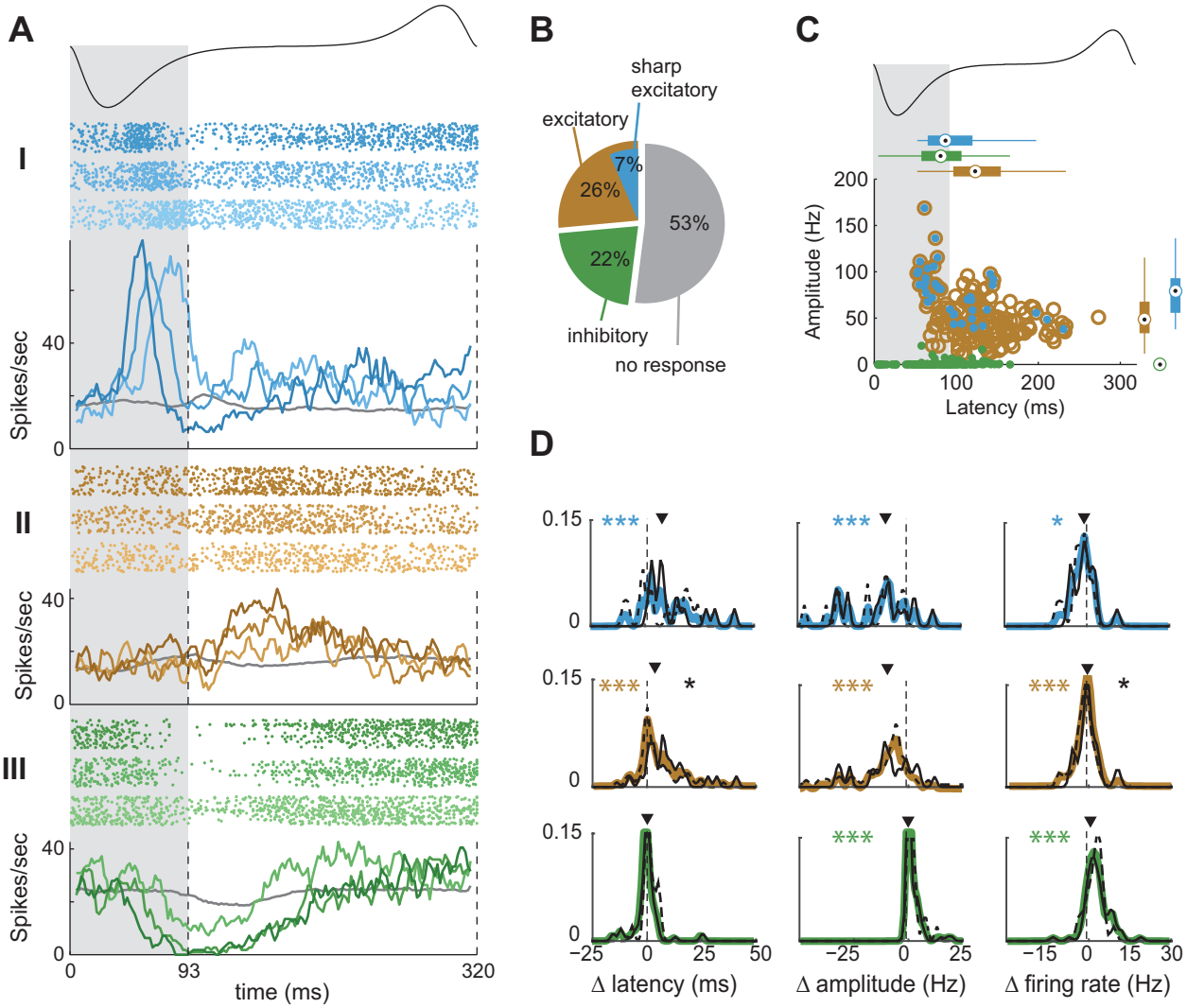

Figure 2.

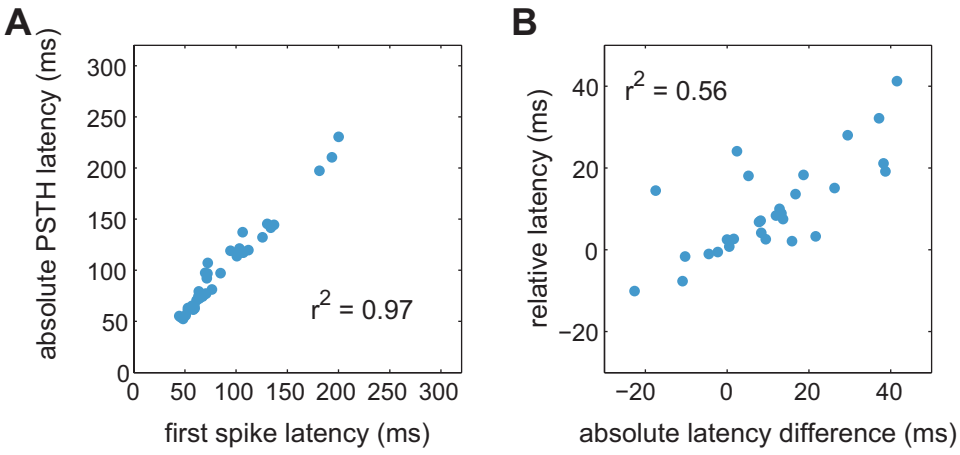

Figure 3.

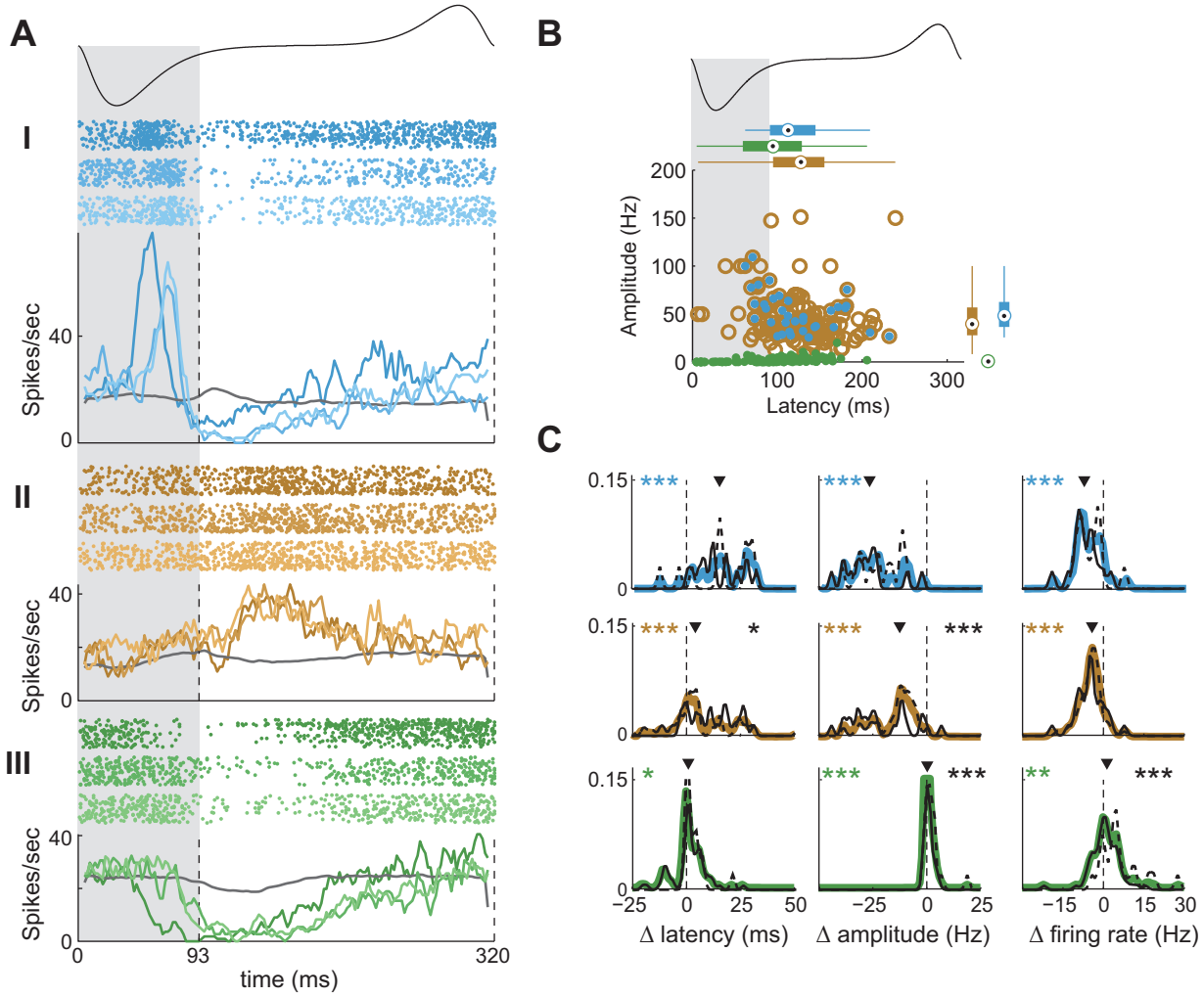

Figure 4.

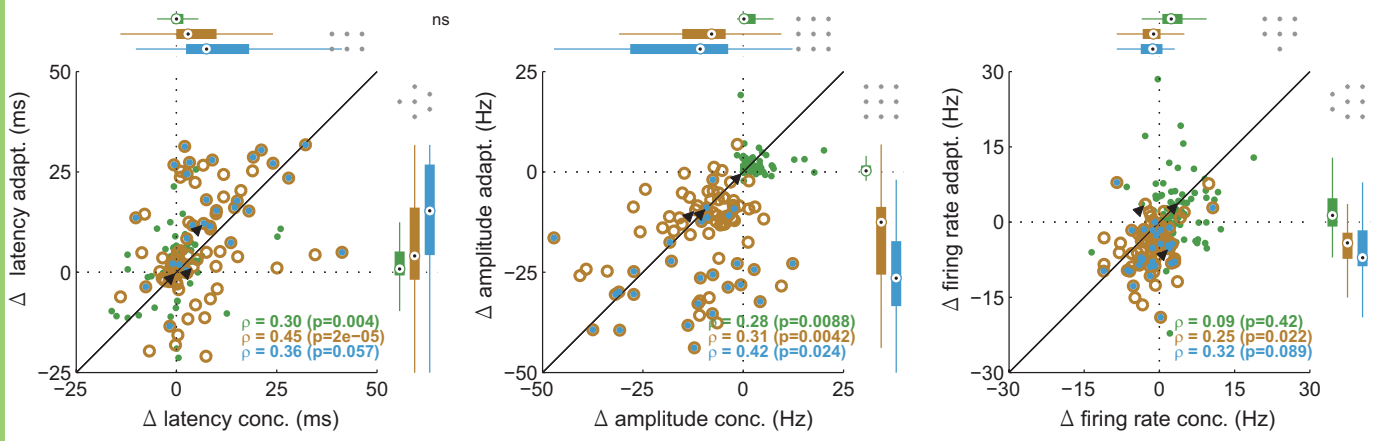

Figure 5

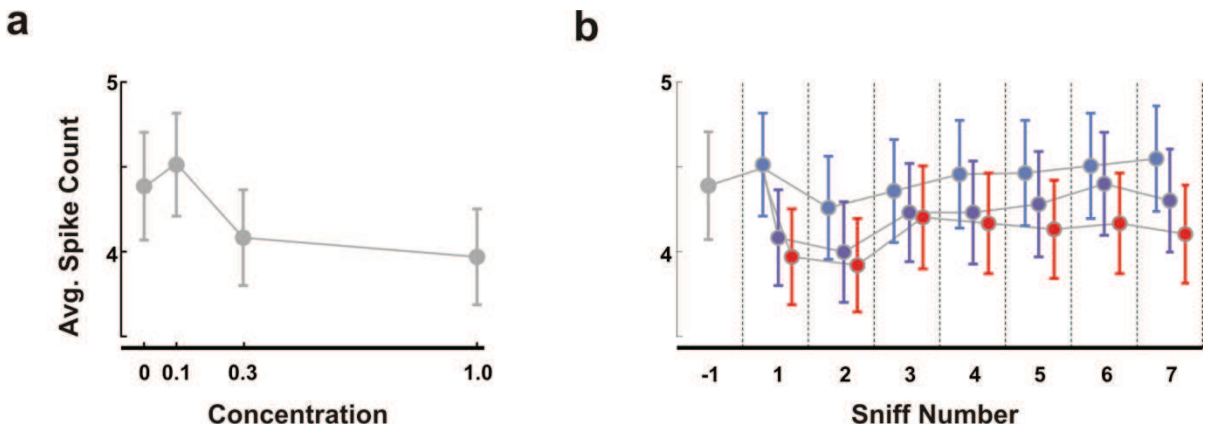

Figure 6.

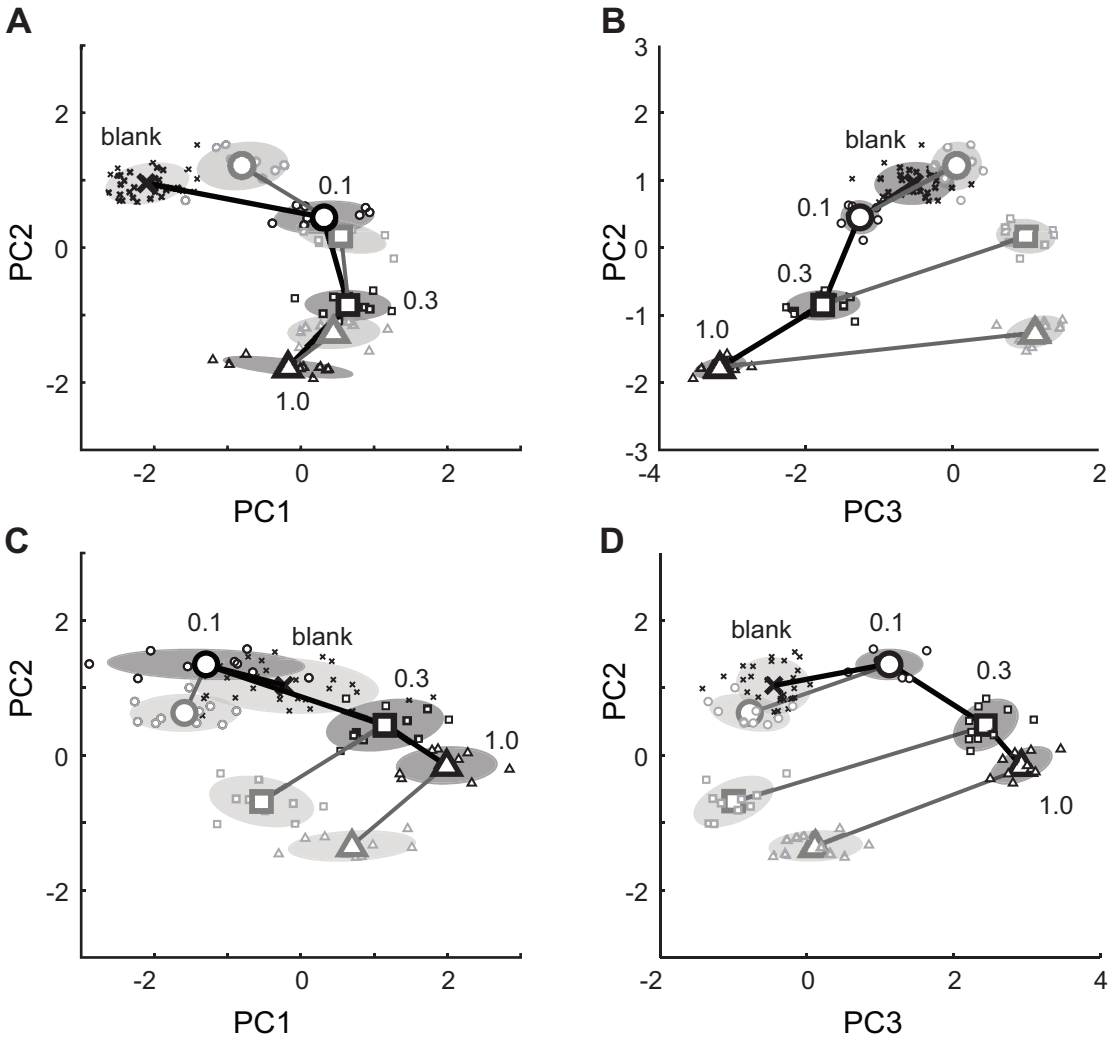

Figure 6.

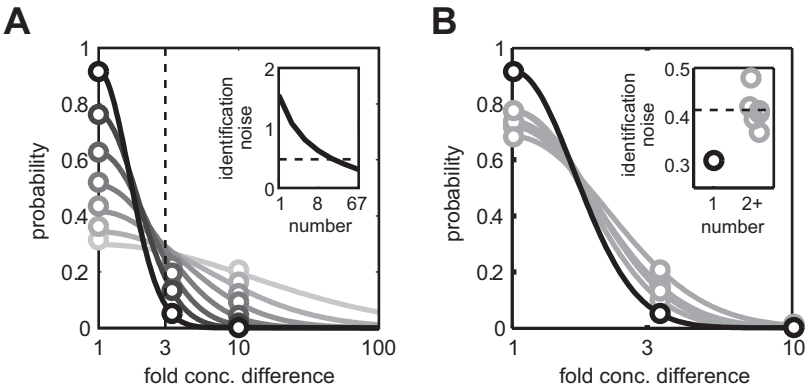

Figure 8.

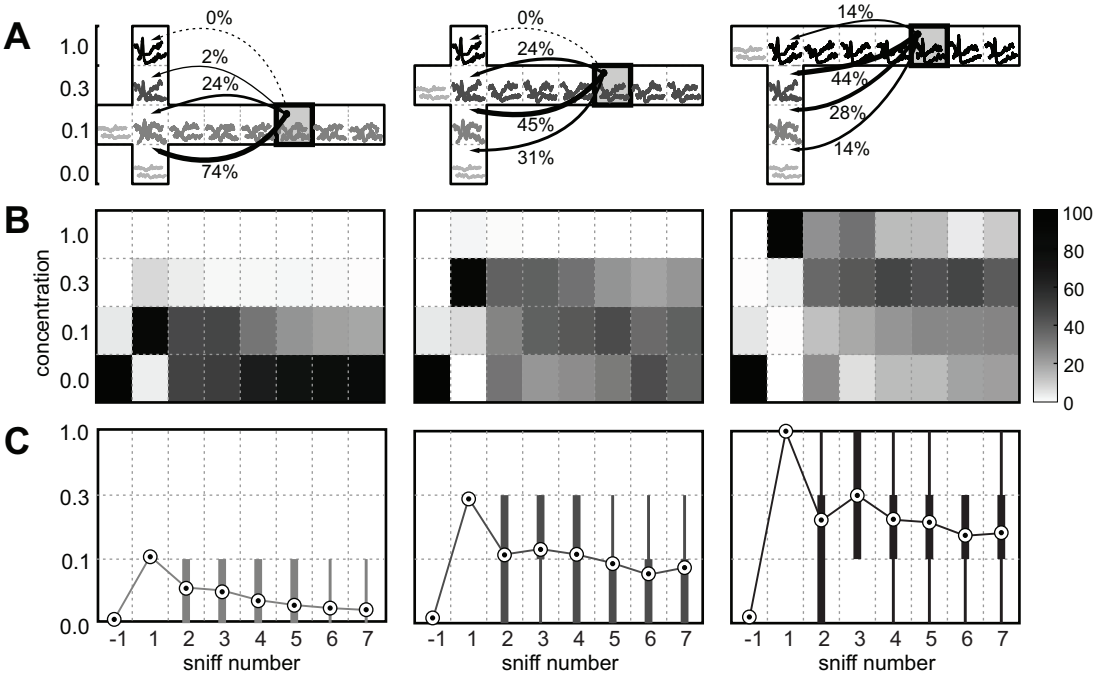

Figure 9.